The Effect of Current Shear on Topographic Rossby Waves

I. L. COLLINGS

Department of Mathematics, Deakin University, Waurn Ponds, Victoria 3217, Australia

R. GRIMSHAW

Department of Mathematics, University of Melbourne, Parkville, Victoria 3052, Australia

(Manuscript received 28 June 1979, in final form 14 September 1979)

ABSTRACT

Topographic Rossby waves are long-period waves which occur on continental slopes. In this paper we examine the effect of a mean current on these waves, when the current is directed along the isobaths and has a linear shear in the transverse direction. Solutions are obtained in terms of Whittaker functions and are applied to some data analyzed by Hamon *et al.* (1975), which has been interpreted as evidence of topographic Rossby waves by Garrett (1979). The modifications due to a linear friction law are also considered.

1. Introduction

When transient motions in a barotropic ocean, such as meanders or eddies, encounter a continental slope, the vortex lines are compressed (or stretched) as they move into regions of shallow (or deep) water, respectively, due to the conservation of potential vorticity. The resulting fluid motion is a topographic Rossby wave whose longshore phase velocity is directed along the isobaths, with the deeper water on the left in the Northern Hemisphere or on the right in the Southern Hemisphere (Le Blond and Mysak, 1978, Section 20). Recently, Garrett (1979) has suggested that data analyzed by Hamon *et al.* (1975) of longshore currents on the East Australian Shelf are consistent with the presence of topographic Rossby waves with an onshore component of group velocity. Kroll and Niiler (1976) have shown that such waves may propagate a considerable distance up the slope before being eliminated by friction. Also, Petrie and Smith (1977) found some evidence for onshore propagation of these waves on the Scotian Shelf.

In this paper we propose to examine the effect of a mean longshore current on topographic Rossby waves. We shall assume that the undisturbed depth is $h(x)$, so that the isobaths are parallel straight lines; the x, y axes are normal to and parallel to the isobaths, respectively (see Fig. 1). The mean longshore current is $v_0(x)$ parallel to the isobaths. Then if $\hat{u}$ and $\hat{v}$ are the x and y components of velocity, respectively, and ζ is the wave height, the governing equations are (Le Blond and Mysak, 1978, Section 20)

$$\left(\frac{\partial}{\partial t} + \hat{u}\frac{\partial}{\partial x} + \hat{v}\frac{\partial}{\partial y}\right)\left(\frac{f+\eta}{H}\right) = 0, \quad (1.1a)$$

$$\frac{\partial H}{\partial t} + \frac{\partial}{\partial x}(H\hat{u}) + \frac{\partial}{\partial y}(H\hat{v}) = 0, \quad (1.1b)$$

where

$$\eta = \frac{\partial \hat{v}}{\partial x} - \frac{\partial \hat{u}}{\partial y}, \quad (1.1c)$$

$$H = h + \zeta. \quad (1.1d)$$

Here f is the Coriolis parameter, and is positive in the Northern Hemisphere but negative in the Southern Hemisphere. Eq. (1.1a) is the equation for conservation of potential vorticity and (1.1b) is the equation for conservation of mass. Hereafter we shall make the nondivergent approximation which means the neglect of ζ compared with h; the approximation is valid when $f^2L^2 \ll gh_0$, where L is the length scale of the waves and h_0 the depth scale. Then the linearized equation for perturbations to the mean longshore current is

$$\left(\frac{\partial}{\partial t} + v_0\frac{\partial}{\partial y}\right)\left[\frac{\partial}{\partial x}\left(\frac{1}{h}\frac{\partial \Psi}{\partial x}\right) + \frac{1}{h}\frac{\partial^2 \Psi}{\partial y^2}\right] - \frac{dP}{dx}\frac{\partial \Psi}{\partial y} = 0, \quad (1.2a)$$

where

$$P(x) = \frac{f + \dfrac{dv_0}{dx}}{h}, \quad (1.2b)$$

0022-3670/80/030363-09$06.25

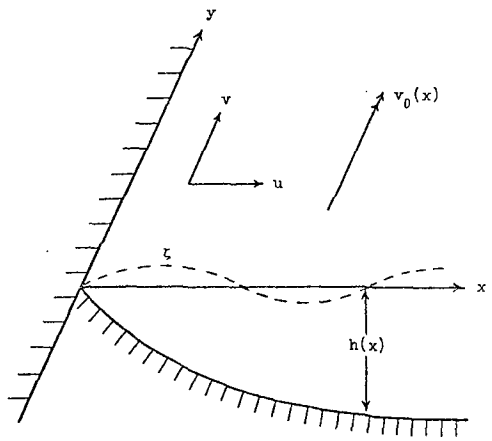

FIG. 1. The coordinate system.

$$hu = \frac{\partial \Psi}{\partial y}, \quad hv = -\frac{\partial \Psi}{\partial x}. \tag{1.2c}$$

Here u and v are the perturbation velocities (i.e., $\hat{u} = u$ and $\hat{v} = v_0 + v$), and Ψ is a streamfunction for the perturbed flow. $P(x)$ is the potential vorticity of the mean current over the slope region. We seek solutions to (1.2a) of the form

$$\Psi = \mathrm{Re}[\psi(x) \exp(imy - imct)], \tag{1.3}$$

where m is the longshore wavenumber and c the longshore phase speed. Substituting (1.3) into (1.2a) it follows that

$$\frac{d}{dx}\left(\frac{1}{h}\frac{d\psi}{dx}\right) - \frac{m^2}{h}\psi + \frac{\psi}{(c - v_0)}\frac{dP}{dx} = 0. \tag{1.4}$$

Our aim is to seek solutions to this equation which describe topographic Rossby waves.

We shall assume throughout that the depth profile is exponential. We let

$$h(x) = h_0 \exp(2\lambda x), \tag{1.5a}$$

$$\psi(x) = h_0^{1/2} \exp(\lambda x)\phi(x). \tag{1.5b}$$

Here we shall assume that λ is positive, so that depth increases with x. Then (1.4) becomes

$$\frac{d^2\phi}{dx^2} - (m^2 + \lambda^2)\phi + \frac{\left[\frac{d^2 v_0}{dx^2} - 2\lambda\left(f + \frac{dv_0}{dx}\right)\right]}{(c - v_0)}\phi = 0. \tag{1.6}$$

Now, if $v_0(x)$ is a constant V, say, a solution of (1.6) is

$$\phi = A \exp(ikx), \tag{1.7a}$$

where

$$c - V = \frac{-2\lambda f}{k^2 + m^2 + \lambda^2} \tag{1.7b}$$

and A is a constant amplitude. Eq. (1.7b) is the dispersion relation for barotropic topographic Rossby waves (Kroll and Niiler, 1976; Garrett, 1979). The intrinsic phase speed $(c - V)$ is such that the wave has the deeper water on the left in the Northern Hemisphere or on the right in the Southern Hemisphere. The corresponding group velocity has components

$$\frac{4\lambda mkf}{(k^2 + m^2 + \lambda^2)^2}, \quad V + \frac{2\lambda(m^2 - k^2 - \lambda^2)f}{(k^2 + m^2 + \lambda^2)^2} \tag{1.8}$$

in the x and y directions, respectively. For onshore propagation we must have $mk < 0$ in the Northern Hemisphere, or $mk > 0$ in the Southern Hemisphere; the constant phase lines $kx + my =$ constant slope offshore from south to north in the Northern Hemisphere, and from north to south in the Southern Hemisphere. The phase lag between two isobaths x_0 and x_1 $(x_0 > x_1)$ is $k(mc)^{-1}(x_1 - x_0)$ units of time.

Hamon *et al.* (1975) have presented two years of data for surface longshore currents on the East Australian shelf, for two alongshore tracks—one 19 km offshore and the other 6.5 km offshore. The data showed a current pattern moving south at a speed of 0.1 m s^{-1}. At the spectral peak at a period of 117 days, the inshore current lagged the offshore current by 10 days. Garrett (1979) has proposed a simple model using the topograhic Rossby wave defined in the previous paragraph. With m and c prescribed (i.e., determined by some fluctuating motion in the deep ocean), Eq. (1.7b) determines k and hence the phase lag can be prescribed. Choosing $V = -0.6$ m s^{-1}, $c = -0.1$ m s^{-1}, $mc = -2\pi$ (117 days)$^{-1}$, $f = -7.3 \times 10^{-5}$ s^{-1}, $\lambda = 2.7 \times 10^{-5}$ m^{-1}, Garrett (1979) found that $k = 8.4 \times 10^{-5}$ m s^{-1} and the phase lag between 19 and 6.5 km is 20 days. The onshore component of group velocity is 6.6×10^{-2} m s^{-1}, and so the time taken for the disturbance energy to travel between the two tracks is 2.2 days; Garrett (1979) shows that this is sufficiently short to allow the disturbance to reach the inshore track before being eliminated by friction. Here V is the mean current in the region between the two tracks, λ the value obtained by Buchwald and Adams (1968) for an exponential fit to the real topography between the two tracks, and f the value for 30°S. Note that V is sufficiently large to ensure that c is negative, although the intrinsic phase speed $c - V$ is positive. The waves are being swept downstream.

The principal purpose of this paper is to modify Garrett's simple model by taking account of the mean current shear. According to Godfrey (1973) this is approximately constant to −30 km offshore, with dv_0/dx approximately equal to -4×10^{-5} s^{-1}. In Section 2 we shall obtain the appropriate solution to (1.6) when v_0 is linear in x up to some value

$x = L$, and is constant for $x > L$. In the application we put $L = 30$ km. We put

$$v_0(x) = \begin{cases} V_0 + \alpha x, & 0 \leq x \leq L \\ V_1, & x \geq L. \end{cases} \quad (1.9)$$

where

$$V_1 = V_0 + \alpha L,$$

Then in $x > L$, we shall suppose that ϕ is given by (1.7a), and k is determined from the dispersion relation (1.7b) with V replaced by V_1. Matching conditions applied at $x = L$ enable this topographic Rossby wave to be continued into the region $x < L$. The matching conditions are continuity of mass flux and wave elevation (Grimshaw, 1976), or in the present case,

$$[\phi]_-^+ = 0, \quad \left[(c - v_0)\frac{d\phi}{dx} + \frac{dv_0}{dx}\phi\right]_-^+ = 0. \quad (1.10)$$

The solution for the case (1.9) is described in Section 2. Note that no boundary condition is imposed at $x = 0$, the shoreline. In this model it is assumed that the wave is eliminated by friction before reaching the shoreline. If this is not the case, there will be some reflection and the solution in $x > L$ would no longer be given by (1.7a). The modifications due to friction are examined in Section 3.

Before proceeding to Section 2, we note that one simple method of incorporating mean current shear is to use the WKB asymptotic solution of (1.6). This is

$$\phi \sim Ak^{-1/2} \exp\left(i \int^x k dx\right), \quad (1.11a)$$

where

$$c - v_0(x) = -\frac{2\lambda(f + \alpha)}{k^2 + m^2 + \lambda^2}. \quad (1.11b)$$

Here k is a function of x determined from the local dispersion relation (1.11b). As x varies from 19 km to 6.5 km, k varies from 8.94×10^{-5} m^{-1} to 17.3×10^{-5} m^{-1}. The phase lag between x_0 and x_1 is now $(mc)^{-1}\int_{x_0}^{x_1} k dx$. With $\alpha = -4 \times 10^{-5}$ s^{-1}, and $v_0(x)$ given by (1.9) (with V_0 chosen so that $v_0 = -0.3$ m s^{-1} at $x_1 = 6.5$ km and $v_0 = -0.8$ m s^{-1} at $x_0 = 19$ km), and the remaining data taking values given in the previous paragraph, we find that the predicted phase lag is 27 days. The time taken for the disturbance energy is obtained by integrating the reciprocal of the onshore component of the group velocity and is 6 days. However, the criterion for the validity of the WKB asymptotic solution is that $|dk/dx| \ll k^2$; with the parameters taking the values given above we find that $|k^{-2}(dk/dx)|$ ranges from 0.59 at $x_1 = 6.5$ km to 0.35 at $x_0 = 19$ km. It is thus doubtful if the WKB approximation will be quantitatively accurate.

Eq. (1.6) has a singularity at x_c, say, where $v_0(x_c) = c$. Near this level the general solution of (1.4) assuming that $dv_0/dx(x_c) \neq 0$, is

$$\phi = [C_1 + aC_2 \ln(x - x_c)](x - x_c)[1 + O(x - x_c)] + C_2[1 + O(x - x_c)], \quad (1.12a)$$

where

$$a = h\frac{dP}{dx}\left(\frac{dv_0}{dx}\right)^{-1}\Big|_{x=x_c} \quad (1.12b)$$

and C_1, C_2 are arbitrary constants. With $v_0(x)$ given by (1.9) and the parameter values described above, there is a singularity at $x_c = 1.5$ km. This is sufficiently close to the shoreline for us to assume that friction will have effectively eliminated the wave before this critical singularity is reached.

Eq. (1.6) also possesses a wave invariant

$$\mathcal{A} = \tfrac{1}{2}\mathrm{Re}\left(i\frac{d\phi}{dx}\bar{\phi}\right) = \tfrac{1}{2}\mathrm{Re}\left(\frac{i}{h}\frac{d\psi}{dx}\bar{\psi}\right), \quad (1.13)$$

as it may readily be shown from (1.6) [or (1.4)] that $\mathcal{A}$ is constant, except at a critical point x_c. Using the conditions (1.10), we see that $\mathcal{A}$ is continuous at $x = L$. $\mathcal{A}$ may be identified as the offshore component of wave action flux, as $\mathcal{A}$ is just the time average of the offshore wave energy flux $h\zeta u$, divided by the intrinsic frequency $m[c - v_0(x)]$. $m\mathcal{A}$ is also the time average of the offshore component of wave momentum flux huv. The time average of the wave energy density $\tfrac{1}{2}h(u^2 + v^2)$ is

$$\frac{1}{4}\left[\left|\frac{d\phi}{dx}\right|^2 + (m^2 + \lambda^2)|\phi|^2 + \lambda\left(\phi\frac{d\bar{\phi}}{dx} + \bar{\phi}\frac{d\phi}{dx}\right)\right].$$

The ratio of $m[c - v_0(x)]\mathcal{A}$ to this quantity determines the velocity of offshore energy propagation. In particular, the sign of $m[c - v_0(x)]\mathcal{A}$ determines the direction of energy propagation. For the case when $v_0(x) = V$, a constant, and ϕ is given by (1.7a), the wave invariant $\mathcal{A}$ is $-\tfrac{1}{2}k|A|^2$, and it is readily verified that the velocity of energy propagation is just the group velocity defined by (1.8). For the case when v_0 is defined by (1.9), $\mathcal{A}$ is again $-\tfrac{1}{2}k|A|^2$ in $x > L$, and hence takes this value for $x < L$, until a singularity is reached. The negative sign shows that there is an onshore flux of wave momentum and wave energy. At a critical point, $\mathcal{A}$ is discontinuous. Determining the branch of the logarithm by replacing mc by $mc + i\epsilon$, $\epsilon > 0$, and taking the limit $\epsilon \to 0$ (this is equivalent to using causality considerations), we find from (1.12) that

$$\mathcal{A} = \begin{cases} \tfrac{1}{2}\mathrm{Re}\,(iC_1\bar{C}_2), & x > x_c \\ \tfrac{1}{2}\mathrm{Re}\,(iC_1\bar{C}_2) \mp \tfrac{1}{2}\pi a|C_2|^2, & x < x_c. \end{cases} \quad (1.14)$$

Here the sign of the second term is determined by the criterion $m(dv_0/dx)(x_c) \lessgtr 0$. The discontinuity in $\mathcal{A}$ at the critical level is $\pm\tfrac{1}{2}\pi a|C_2|^2$; for the param-

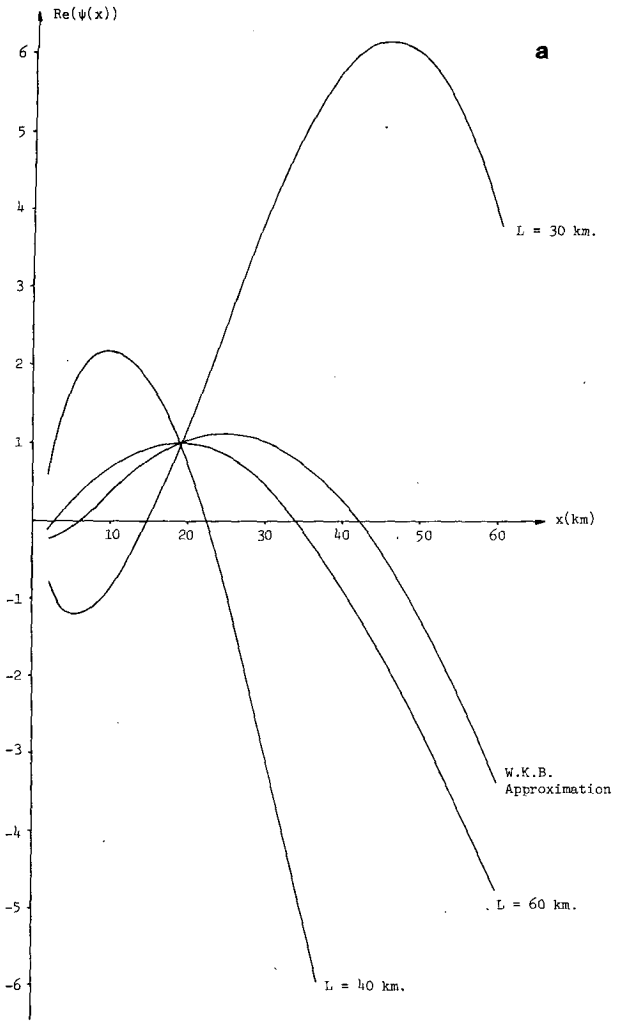

FIG. 2a. A plot of Re $[\psi(x)]$ versus x for $L = 30$, 40 and 60 km, compared with the WKB approximation. All plots are normalized so that $\psi(19\text{ km}) = 1$.

eter values quoted above, this is negative, showing that the wave action flux, or wave momentum flux, being directed toward $x = x_c$ from the offshore side is absorbed at the critical level. The wave momentum flux divergence is $\pm\frac{1}{2}\pi am|C_2|^2\delta(X - X_c)$, where δ is the Dirac delta function, and hence has the correct sign to support a positive longshore pressure gradient (cf. Garrett, 1979).

2. Solution for constant mean current shear

With $v_0(x)$ given by (1.9) the solution in $x > L$ is

$$\phi = A_1 \exp[ik_1(x - L)], \tag{2.1a}$$

where

$$c - V_1 = -\frac{2\lambda f}{(k_1^2 + m^2 + \lambda^2)}. \tag{2.1b}$$

For the region $0 < x < L$, the governing equation is (1.6) or

$$\frac{d^2\phi}{dx^2} - (m^2 + \lambda^2)\phi - \frac{2\lambda(f + \alpha)}{(c - V_0 - \alpha x)}\phi = 0. \tag{2.2}$$

From (1.10) and (2.1a) the boundary conditions at $x = L$ (as $x \to L$ from below) are

$$\phi|_{x=L} = A_1, \quad \left.\frac{d\phi}{dx}\right|_{x=L} = \nu A_1, \tag{2.3a}$$

where

$$\nu = ik_1 - \frac{\alpha}{c - V_1}. \tag{2.3b}$$

Putting

$$z = \beta(c - V_0 - \alpha x), \quad \alpha^2\beta^2 = 4(\lambda^2 + m^2) \tag{2.4a}$$

and

$$\kappa = -\frac{\beta\lambda(f + \alpha)}{2(\lambda^2 + m^2)}, \tag{2.4b}$$

it may be shown that Eq. (2.2) becomes

$$\frac{d^2\phi}{dz^2} + \left(-\frac{1}{4} + \frac{\kappa}{z}\right)\phi = 0. \tag{2.5}$$

This is just Whittaker's equation (Abramowitz and Stegun, 1964, Chap. 13) and two linearly independent solutions are

$$\phi_1(z) = M_{\kappa,1/2}(z), \quad \phi_2(z) = W_{\kappa,1/2}(z), \tag{2.6}$$

where $M_{\kappa,\mu}(z)$ and $W_{\kappa,\mu}(z)$ are Whittaker functions. $M_{\kappa,1/2}(z)$ and $W_{\kappa,1/2}(z)$ are in turn the product of $z\exp(-z/2)$ with the Kummer functions $M(1 - \kappa, 2, z)$ and $U(1 - \kappa, 2, z)$. $\phi_1(z)$ is a regular function of z, while $\phi_2(z)$ has a logarithmic singularity at $z = 0$. Thus we may put

$$\phi = A_1\{B_1\phi_1(z) + B_2\phi_2(z)\}, \tag{2.7}$$

where B_1, B_2 are constants determined from the boundary conditions (2.3a). We find that

$$\alpha\beta WB_1 = \alpha\beta\left.\frac{d\phi_2}{dz} + \nu\phi_2\right|_{x=L}, \tag{2.8a}$$

$$\alpha\beta WB_2 = -\alpha\beta\left.\frac{d\phi_1}{dz} - \nu\phi_1\right|_{x=L}, \tag{2.8b}$$

where

$$W = \phi_1\frac{d\phi_2}{dz} - \phi_2\left.\frac{d\phi_1}{dz}\right|_{x=L}. \tag{2.8c}$$

Here W is the Wronskian of the solutions ϕ_1 and ϕ_2, and is $\{\kappa\Gamma(-\kappa)\}^{-1}$. All the numerical results quoted in this section are for the parameter values given in Section 1; we find that $\beta = 1.38\text{ s m}^{-1}$ and $\kappa = 2.75$; z ranges from 1.58 at $x = 30$ km to 0.97 at $x = 19$ km and 0.28 at $x = 6.5$ km. The Whittaker functions are evaluated from the power series expansions in z of the Kummer functions (Abramowitz and Stegun, 1964, Chap. 13). Fig. 2a shows a plot of Re (ψ) against x for $L = 30$, 40 and 60 km. All plots are normalized

so that $\psi(x = 19 \text{ km}) = 1$. Note that the apparent change of sign between the case $L = 30$ km and $L = 40$ km is an artifact of this normalization. Replotting the curves with the normalization $\psi(x = L \text{ km}) = 1$, for example, would produce a quite different picture (see Fig. 2b). Hereafter, all results will be for $L = 30$ km unless otherwise specifically stated.

The WKB approximation of Section 1 can be rederived from the solution (2.7) and (2.8) by using the asymptotic form of the Whittaker functions as $\kappa \to \infty$ (Abramowitz and Stegun, 1964, Chap. 13). The result is

$$\phi \approx A_1\left(\frac{z}{z_L}\right)^{1/4} \exp[2i(\kappa z_L)^{1/2} - 2i(\kappa z)^{1/2}], \quad (2.9)$$

where z_L is the value of z when $x = L$. This agrees with the result obtained when (1.11a) is used in conjunction with the boundary conditions (2.3a); note that the wavenumber $k \approx \alpha\beta(\kappa/z)^{-1/2}$. Fig. 2a shows a plot of Re ψ using the WKB asymptotic solution (2.9) and comparing this with the true solution. It is apparent that increasing the value of L brings the true solution closer to the WKB asymptotic solution, but that for $L = 30$ km, the true solution must be used. The validity of the WKB asymptotic solution requires $(\kappa z)^{1/2} \gg 1$, and this may be achieved by increasing L. However, note that the WKB solution fails as $z \to 0$ (or $x \to x_c$); this is easily seen by comparing (2.9) with (1.12a). Since $x_c = 1.5$ km in our case, and we require the solution to be valid down to $x = 6.5$ km, this is an additional reason why the true solution must be used.

The total streamfunction is

$$\hat{\psi}(x,y,t) = -\int_{x_0}^{x} hv_0 dx + \text{Re}\,[\psi(x)\exp(imy - imct)], \quad (2.10)$$

and the total longshore velocity component is

$$\hat{v}(x,y,t) = v_0(x) + \text{Re}\left[-\frac{1}{h}\frac{d\psi}{dx}\exp(imy - imct)\right]. \quad (2.11)$$

Here $\psi(x)$ is related to $\phi(x)$ by (1.5b) and $\phi(x)$ is given by (2.7) and (2.8). The function $\phi(x)$ contains an arbitrary constant A_1. The data presented by Hamon *et al.* (1975) show that the fluctuations in the longshore current are comparable to the magnitude of the mean current. Hence, we choose A_1 so that the perturbation velocity v at $x = 19$ km has a minimum value equal to $v_0(x = 19 \text{ km})$ or -0.8 m s^{-1}. Fig. 3a shows a contour plot of $\hat{\psi}$ for $t = 0$; this streamline pattern (for the mass transport) propagates southward at a speed of 0.1 m s^{-1}. Our solution shows a series of large meanders with a longshore wavelength 2π m^{-1} or ~1000 km, and an offshore wavelength of ~50 km. Fig. 3b shows the corresponding contour plot when $v_0(x) = V$, a constant, and ϕ is then given by (1.7a); the offshore wave-

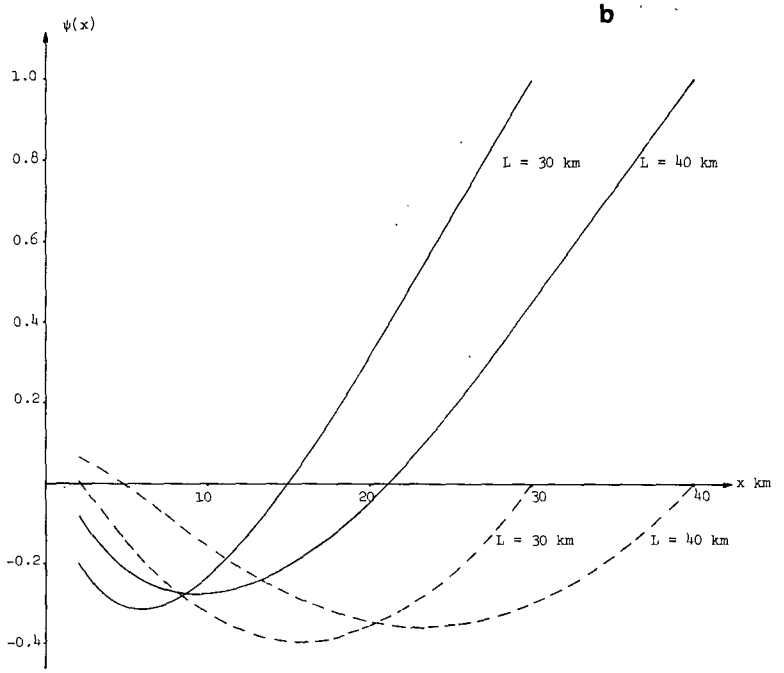

FIG. 2b. Plots of Re $[\psi(x)]$ (——) and Im $[\psi(x)]$ (– – –) for $L = 30$ and 40 km. Both plots are normalized so that $\psi(x = L) = 1$.

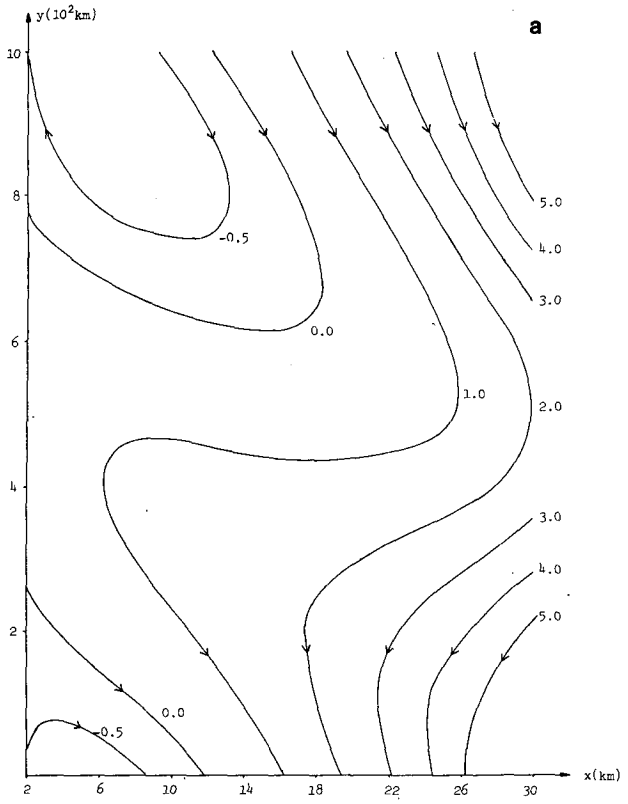

FIG. 3a. A contour plot of the total streamfunction $\hat{\psi}$ for $t = 0$ when $v_0(x)$ is given by (1.9) with $L = 30$ km; the units are 10^6 m^3 s^{-1}.

length in this case is ~75 km. Fig. 4a shows a contour plot of $\hat{v}$ for t = constant, while Fig. 4b shows the corresponding contour plot when $v_0(x) = V$. Note that one effect of including the shear in the basic velocity profile is to intensify the inshore northward currents. From (2.11) we see that

$$\hat{v}(x,y,t) = v_0(x) - a(x)\cos[my - mct + \epsilon(x)], \quad (2.12a)$$

where

$$a(x) = \left|\frac{1}{h}\frac{d\psi}{dx}\right|, \quad (2.12b)$$

$$\epsilon(x) = arg\left[\frac{1}{h}\frac{d\psi}{dx}\right]. \quad (2.12c)$$

It follows that the phase lag between two isobaths x_0 and x_1 is $(mc)^{-1}[\epsilon(x_1) - \epsilon(x_0)]$ units of time. In Fig. 5 we show a plot of this quantity for $x_0 = 19$ km as x_1 varies. When $x_1 = 6.5$ km, the phase lag is 29 days. This is for a period of 117 days corresponding to the observed spectral peak. For waves of a lower period, the value of m is increased, but provided m remains significantly smaller than λ, our solutions for ϕ are not significantly altered and so the phase $\epsilon(x)$ is not significantly altered; thus since the phase lag is proportional to the period, a lower period will produce a lower phase lag. Finally, using the definitions given in the last paragraph of Section 1 we can determine the velocity of energy propagation as a function of x, and hence show that the travel time for a distance to travel from $x_0 = 19$ km to $x_1 = 6.5$ km, is 3.6 days. Also, we find that $m\mathscr{A}$ (the time average of the offshore component of wave momentum flux) is -0.88 m^3 s^{-2}; by contrast the discontinuity in $m\mathscr{A}$ (1.14) at $x = x_c$ (here $x_c = 1.5$ km) is -2.7 m^3 s^{-2}. This latter wave momentum flux divergence could support a longshore pressure gradient of 1.4×10^{-6} m s^{-2}, whereas the observed longshore pressure gradient is 5×10^{-6} m s^{-2} (Garrett, 1979).

3. Modifications due to friction

The theory described in Section 2 not only predicts a phase lag larger than the observed value, but also predicts larger currents inshore than the observed currents, which are smaller on the inshore track ($x = 6.5$ km) by a factor of 2 (Hamon *et al.*, 1975). Garrett (1979) has discussed a number of effects which may act to improve the predicted values. Here we propose to discuss just the modifications to our theory due to friction.

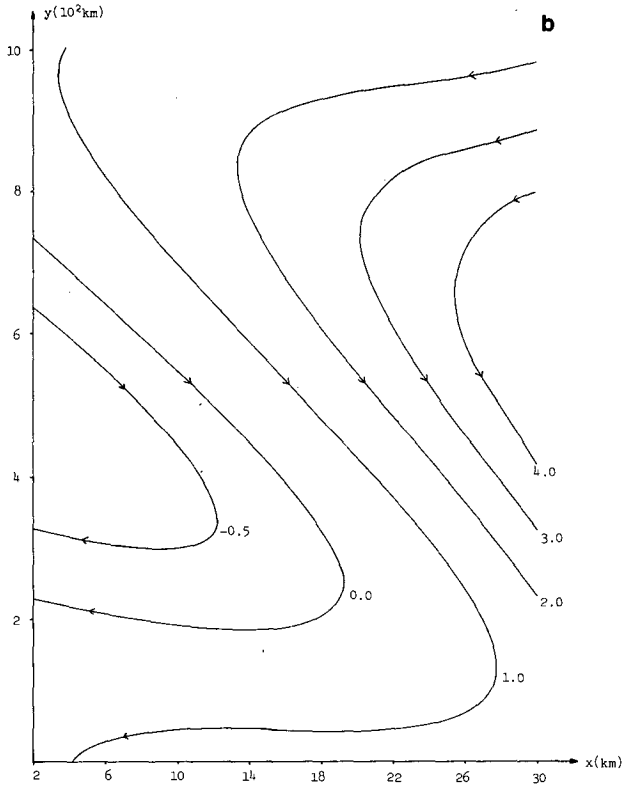

FIG. 3b. The corresponding contour plot when $v_0(x) = V(-0.6$ m s$^{-1})$.

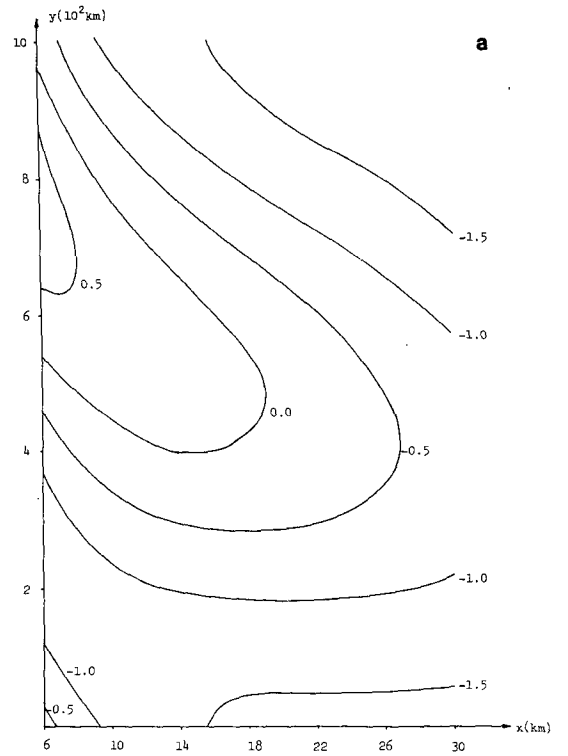

FIG. 4a. A contour plot of the total longshore velocity $\hat{v}$ for $t = 0$ when $v_0(x)$ is given by (1.9) with $L = 30$ km; the units are m s^{-1}.

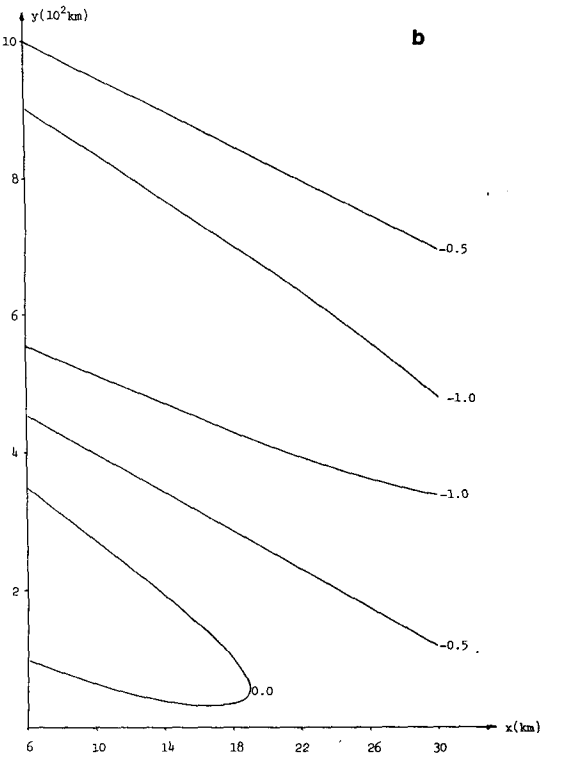

FIG. 4b. The corresponding contour plot when $v_0(x) = V(-0.6$ m s$^{-1})$.

To include friction in our model, we introduce stresses $\tau^{(x)}$ and $\tau^{(y)}$ in the x and y momentum equations, respectively. Then the potential vorticity equation (1.1a) is modified by the presence of a term

$$\frac{1}{H}\left[\frac{\partial \tau^{(x)}}{\partial y} - \frac{\partial \tau^{(y)}}{\partial x}\right] \tag{3.1}$$

on the right-hand side, while (1.1b) remains unchanged. We follow the procedure of Kroll and Niiler (1976) and assume a linear friction law

$$\tau^{(x)} = \gamma(x)u, \quad \tau^{(y)} = \gamma(x)v. \tag{3.2}$$

Then (1.4) is modified by the presence of a term

$$-\frac{i}{m(c - v_0)}\left[\frac{d}{dx}\left(\frac{\gamma}{h}\frac{d\psi}{dx}\right) - \frac{m^2\gamma}{h}\psi\right]. \tag{3.3}$$

Kroll and Niiler (1976) have argued that if the friction is principally due to bottom friction, then γ is proportional to h^{-1} (typical bottom velocity). Since a typical bottom velocity will vary as $h^{-1/2}$, γ is proportional to $h^{-3/2}$. This makes the differential equation difficult to solve by simple analytic means. Here, for simplicity, we shall suppose that γ is a constant. Using the values quoted by Kroll and Niiler for γ and averaging their results over all depths between $x = 6.5$ km and $x = 19$ km, we put $\gamma = 2.2 \times 10^{-6}$ s^{-1}. This is smaller than the value used by Garrett (1979), whose estimate was based on the assumption that the typical bottom velocity has a magnitude comparable with the mean surface velocity; this is almost certainly an overestimate. With γ a constant, Eq. (1.4) is modified merely by replacing c by $c + i\gamma m^{-1}$. Thus the solutions in Section 1 and 2 will remain unchanged except for a time decay factor of $\exp(-\gamma t)$. From a knowledge of the time for the disturbance to travel from x_0 to x_1, we can compute a frictional decay factor, and compare this with the amplitude increase in the absence of friction.

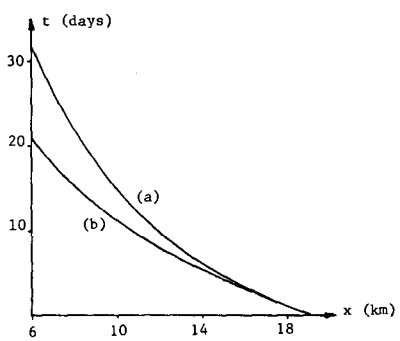

FIG. 5. A plot of the phase lag when $v_0(x)$ is given by (1.9), with $L = 30$ km: (a) no friction, (b) in the presence of friction.

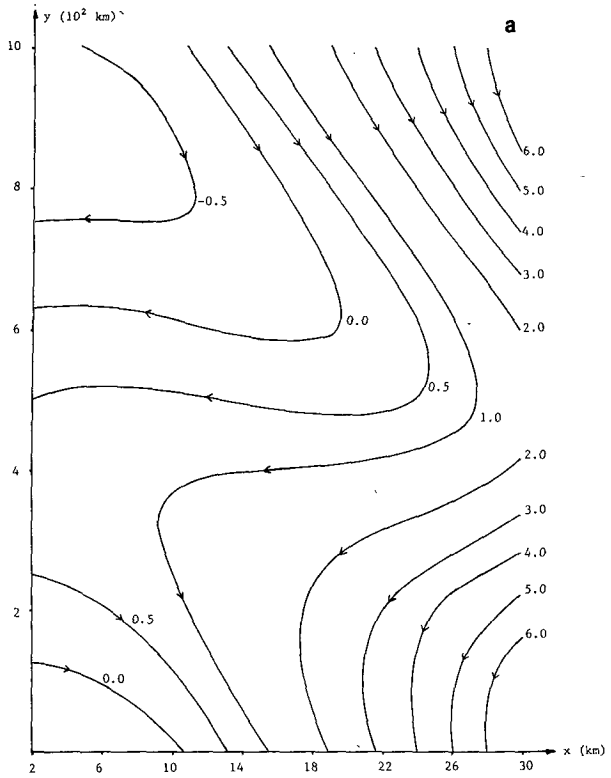

FIG. 6a. A contour plot of the total streamfunction $\hat{\psi}$ for $t = 0$ when $v_0(x)$ is given by (1.9) with $L = 30$ km in the presence of friction; the units are 10^6 m^3 s^{-1}.

However, it is not obvious that the effect of friction is to impose a spatially uniform time decay on the wave. It is more likely to generate a decay in the x direction. Thus for the case when $v_0(x) = V$, the dispersion relation (1.7b) with c replaced by $c + i\gamma m^{-1}$ will have a complex-valued solution for k, $k_0 - i\delta$, say; consequently, the solution (1.7a) will contain a decay factor of $\exp(\delta x)$. This decay factor will agree with that calculated using a time decay factor only when γ is small compared to $m(c - V)$, as then γ is approximately δ(x component of group velocity). In the present case γ is comparable with $m(c - V)$. We find $k_0 = 7.2 \times 10^{-5}$ m^{-1} and $\delta = 2.6 \times 10^{-5}$ m^{-1}. The phase lag between 19 and 6.5 km is now 17 days, and the frictional decay factor is 0.72. The amplitude increase is proportional to $h^{-1/2}$ and gives a factor of 1.4; together there is virtually no decay. Thus the effect of a uniform coefficient of friction is to bring Garrett's (1979) simple model closer to agreement with the data, both with respect to the phase lag and the current amplitudes. A larger value of γ would tend to decrease the phase lag further.

For the WKB approximate solution, the dispersion relation (1.11b) is modified by replacing c on the left-hand side by $c + i\gamma m^{-1}$. The wavenumber $k = k_0 - i\delta$ determined from (1.11b) is a function of x and substitution into (1.11a) determines the phase lag $(mc)^{-1}\int_{x_1}^{x_0} k_0 dx$ and the decay factor $\exp(-\int_{x_1}^{x_0} \delta dx)$. As x varies from 19 to 6.5 km, k_0 varies from 8.2×10^{-5} to 10.4×10^{-5} m^{-1}, and δ varies from 2.1×10^{-5} to 6.3×10^{-5} m^{-1}. We find a predicted phase lag of 22 days, and a decay factor of 0.63. For this case the amplitude increase is proportional to $(k^2 + \delta^2)^{1/2}h^{-1/2}$, and gives a factor of 2.0; together there is an amplitude increase of 1.26.

Next, we turn to the case when $v_0(x)$ is given by (1.9) when the solution for ϕ is (2.7) and (2.8) with c replaced by $c + i\gamma m^{-1}$. This causes no changes in β and κ, but z (2.4a) becomes a complex variable, with a constant imaginary part. The Whittaker functions may be evaluated numerically as before, using power series expressions for the Kummer functions. Fig. 6a shows a contour plot of the total streamfunction $\hat{\psi}$ for $t = 0$, while Fig. 6b shows a contour plot of the total longshore velocity $\hat{v}$ for $t = 0$; the corresponding plots in the absence of friction are Figs. 3a and 4a, respectively. They show that the effect of friction is to slightly inhibit the onshore incursion of the meander, with the consequence that the inshore regions of northward current are displaced slightly offshore. The phase lag is plotted in

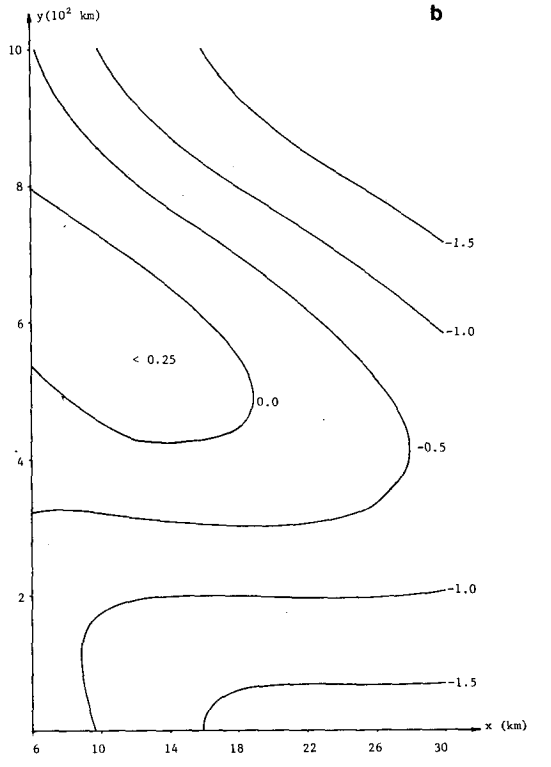

FIG. 6b. A contour plot of the total longshore velocity $\hat{v}$ for $t = 0$ when $v_0(x)$ is given by (1.9) with $L = 30$ km in the presence of friction; the units are m s^{-1}.

TABLE 1. A tabulation of the predicted phase lag between $x = 19$ km and $x = 6.5$ km for the various cases discussed in the text with and without the effects of friction.

	$v_0(x)$	$\phi(x)$	Friction coefficient $\gamma = 0$	Friction coefficient $\gamma = 2.2 \times 10^{-6}$ s^{-1}
Phase Lag (in days)	Constant $V = 0.6$ m s^{-1}	(1.7a)	20	17
	Linear shear Eq. (1.9)	WKB (1.11a)	27	22
	Linear shear Eq. (1.9)	Exact (2.7)	29	19

Fig. 5, and is 19 days for the interval from $x_0 = 19$ km to $x_1 = 6.5$ km. Note that as x increases $m[c - v_0(x)]$ increases relative to γ, and so the relative effect of friction is more pronounced inshore. Also, increasing the value of γ decreases the phase lag; for example, if $\gamma = 3.1 \times 10^{-6}$ s^{-1}, the phase lag is 15 days. All our results for phase lags are tabulated in Table 1.

REFERENCES

Abramowitz, M., and I. A. Stegun, 1964: *Handbook of Mathematical Functions. NBS Appl. Math. Ser.*, Vol. 55, Washington, DC, 1046 pp.

Buchwald, V. T., and J. K. Adams, 1968: The propagation of continental shelf waves. *Proc. Roy. Soc. London*, **A305,** 235–250.

Garrett, C., 1979: Topographic Rossby waves off East Australia: Identification and role in shelf circulation. *J. Phys. Oceanogr.*, **9,** 244–253.

Godfrey, J. S., 1973: Comparison of the East Australian Current with the western boundary flow in Bryan and Cox's (1968) numerical model ocean. *Deep-Sea Res.*, **20,** 1059–1076.

Grimshaw, R., 1976: The stability of continental shelf waves in the presence of boundary current shear. School of Math. Sci., Res. Rep. No. 46, University of Melbourne, 20 pp.

Hamon, B. V., J. S. Godfrey and M. A. Greig, 1975: Relation between mean sea level, current and wind stress on the east coast of Australia. *Aust. J. Mar. Freshwater Res.*, **26,** 389–403.

Kroll, J., and P. P. Niiler, 1976: The transmission and decay of barotropic topographic Rossby waves incident on a continental shelf. *J. Phys. Oceanogr.*, **6,** 432–450.

Le Blond, P. H., and L. A. Mysak, 1978: *Waves in the Ocean. Elsevier Oceanogr. Ser.*, Vol. 20, 602 pp.

Petrie, B., and P. C. Smith, 1977: Low-frequency motions on the Scotian shelf and slope. *Atmosphere*, **15,** 117–140.